IEEE Access
Multidisciplinary ⋮ Rapid Review ⋮ Open Access Journal

Received 9 November 2023, accepted 22 November 2023, date of publication 23 November 2023,
date of current version 20 December 2023.

Digital Object Identifier 10.1109/ACCESS.2023.3336420

APPLIED RESEARCH

Influence of Spherical Aberration on the SNR in Single-Beam Laser Doppler Velocimeter for Remote Measurement

LANJIAN CHEN, JIAN ZHOU, CHONGBIN XI, XIAOMING NIE, AND SHILONG JIN

College of Advanced Interdisciplinary Studies, National University of Defense Technology, Changsha 401173, China
Nanhu Laser Laboratory, National University of Defense Technology, Changsha 401173, China

Corresponding author: Jian Zhou (wttzhoujian@163.com)

This work was supported by the Natural Science Foundation of Hunan Province, China, under Grant 2021JJ30782.

ABSTRACT In contrast to those deployed on land vehicles, the single-beam Laser Doppler velocimeter (LDV) used for velocity acquisition on airborne vehicles requires a focusing transmitter. The effects of spherical aberration in focusing transmitters on the distant velocity measurement of single-beam Laser Doppler velocimeters are demonstrated in this work. The calculations of the numerical simulations based on the generated theories and the subsequent experiments are in agreement with the theoretical analyses. The impact of spherical aberration on the signal-to-noise ratio (SNR) of single-beam Laser Doppler velocimeters is explained. Also illustrated is the generalized analysis for single-beam Laser Doppler velocimeters equipped with complex optics. An efficient approach for evaluating and advancing the SNR performance of single-beam Laser Doppler velocimeters used for distant velocity measurement is demonstrated. Works in this paper pave way for the design of airborne LDV.

INDEX TERMS Aberration, laser Doppler velocimeter (LDV), remote velocity measurement, SNR.

I. INTRODUCTION

Single-beam Laser Doppler Velocimeter (LDV) technology has advanced significantly, offering high precision, outstanding dependability, and a broad dynamic range for the measurement of ground vehicle velocities [1], [2], [3], [4], [5]. Applications requiring precise velocity measurement have recently arisen, including the integrated navigation of unmanned aerial vehicles (UAVs) and the landing navigation of spacecraft [6], [7], [8]. However, GNSS-denied (global navigation satellite system) conditions resulting in the loss of velocity information are frequently experienced by airborne vehicles because of the occlusion of buildings and trees. The localization accuracy of air vehicles could be significantly increased if LDVs are put on them for continuous and precise velocity monitoring. The low working distance of single-beam LDVs now in use is a general drawback that makes it challenging to use them in airborne vehicles for velocity collection. So it is desirable to increase the working range of single-beam LDVs to hundreds or even kilometers.

Single-beam LDVs are ideal for use on low-altitude air vehicles thanks to research by our group [9] that shows how the probe beam of LDVs may be focused to the required distance using a beam transformation device before it illuminates the targets. Figure 1 illustrates the structure of the focusing transmitter. There is an adjustable distance Δ between the focus points of the two lenses. By manipulating the Δ, the probe beam can be focused on any target. Additionally, the beam is collimated and extended with a ratio equal to the ratio of the focus of the two lenses when the Δ is zero.

The effect of single-lens aberrations on laser beams has been covered in several earlier studies [10], [11], [12], although there are inherent aberrations associated with lenses, such as spherical aberration, coma, and astigmatism. Analysing the degree of SNR change in the remote measurement brought on by aberrations in the focusing transmitter is crucial to ensure effective measurement of the single-beam LDV as the measurement SNR already decreases with the increase of working distance. Since the transmitters of

The associate editor coordinating the review of this manuscript and approving it for publication was Bo Pu.

© 2023 The Authors. This work is licensed under a Creative Commons Attribution-NonCommercial-NoDerivatives 4.0 License.
For more information, see https://creativecommons.org/licenses/by-nc-nd/4.0/

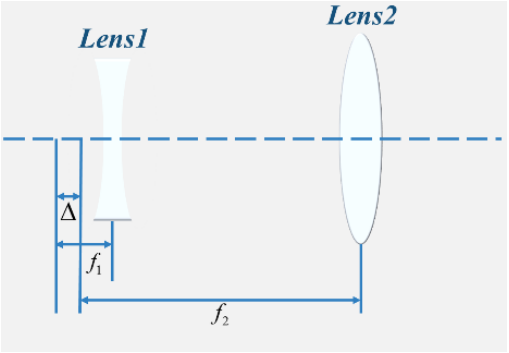

FIGURE 1. The structure of the focusing optics module.

single-beam LDVs are coaxial, the spherical aberration of lenses needs to be taken into specific consideration. Astigmatism and coma are examples of aberrations that do not pose any problems because they disappear on the axis [13].

In particular, the influence of the spherical aberration on the remote measurement of single-beam LDVs is illustrated in this work. The field intensity distribution formulas for the output plane of the focusing transmitter are developed in Section II, accounting for spherical aberration as a phase factor. Then, in Section III, we present the numerical simulations for focusing transmitters made up of various lenses. Last but not least, the experimental results are presented in Section IV which essentially validates the theoretical approach. Works presented here provide an efficient approach for improving the performance of airborne LDV.

II. THEORY

A. THE SNR EXPRESSION FOR SINGLE-BEAM LDVS

The signal-to-noise ratio (SNR) is a commonly used metric to assess how well signal measurements are performing. Consider a volume *V(x,y,z)* of random diffuse scatters at the target position, the SNR expression is given by [14]

$$SNR = \frac{\eta}{h\nu BF_h}\lambda^2 \int_0^\infty P\left(t - \frac{2z}{c}\right) T^2(z)\, dz \cdot \iint \beta(x,y,z) I_{nx}(x,y,z)\, I_{nb}(x,y,z)\, dxdy \quad (1)$$

where η is the optical efficiency of optics in LDVs, F_h and B are the detector's noise factor and noise-equivalent bandwidth in single-beam LDVs respectively, and P and T represent the output power and the one-way transmission efficiency of the probe beam of LDVs.

Eq. (1) is a universal formula for the analysis of SNR in Doppler wind Lidar (DWL). Instead of soft targets like aerosol particles in DWL, single-beam LDVs are thought of for the velocity measurement of carriers. Hence, β is given by

$$\beta(x,y,z) = \delta(z - L)\,\rho(x,y) \quad (2)$$

where ρ is the density of scatters on the target plane. In this case, the integral is written as

$$SNR = \frac{\eta}{h\nu BF_h}\lambda^2 P\left(t - \frac{2L}{c}\right) T^2(L) \cdot \iint \rho(x,y) I_{np}(x,y,z)\, I_{nb}(x,y,z)\, dxdy \quad (3)$$

I_{np} and I_{nb} are the target plane irradiances of the probe and back propagated beams normalized by their total power which is given by

$$I_{np}(x,y,z) = I_{nb}(x,y,z) = \frac{1}{S} \quad (4)$$

where S is the area of the probe beam on the target plane. As the beam is focused on the target by the coaxial focusing transmitter, it is anticipated that the probe beam's spot will have a circular shape.

Using

$$S = \pi \cdot r^2 \quad (5)$$

where r is the radius of the focused probe beam on the target plane. Eventually, Eq. (3) is simplified to

$$SNR = \frac{\eta}{\pi h\nu BF_h}\lambda^2 P\left(t - \frac{2L}{c}\right) T^2(L)\frac{\rho}{r^2} \quad (6)$$

It is possible to obtain the SNR expression of single-beam LDVs using a focusing transmitter. It means that for a given LDV and focused probe beam radius on the target plane at a given working distance, a measurement with a higher SNR will be obtained.

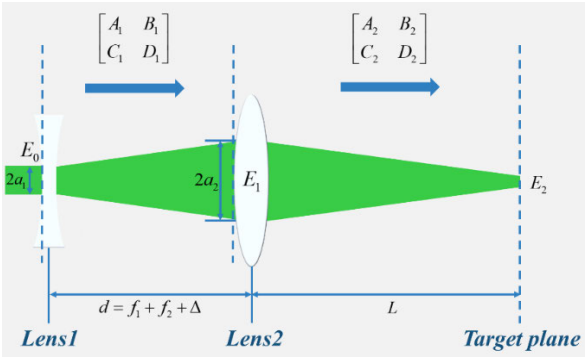

FIGURE 2. The process of the probe beam passing through the focusing optics module.

B. THE INFLUENCE OF SPHERICAL ABERRATION ON THE PROBE BEAM

LDV probe beams typically focus on the target plane after passing through two lenses in a focusing transmitter. This process is depicted figuratively in Fig. 2. Therefore, in the first step, the probe beam is transmitted from the input plane of *Lens1* to the front plane of *Lens2*, which is described by the

diffraction integral relating the fields across these two planes given by

$$E_1(r_1, d) = \frac{i}{\lambda B_1} e^{-ikd} \int_0^{2\pi} \int_0^{a_1} E_0(r_0, 0) \cdot e^{-\frac{ik}{2B_1}\left(A_1 r_0^2 - 2r_1 r_0 \cos(\theta_1 - \theta_0) + D_1 r_1^2\right)} r_0 dr_0 d\theta_0 \quad (7)$$

Which is based on the Collins formula and under the Paraxial approximation [15]. E_1 represents the field distribution at the front plane of *Lens2* as E_0 for the one at the input plane of *Lens1*. a_1 stands for the radius of the input probe beam. k is the wavenumber of the wavelength λ of the probe beam. d is the axial optical distance between the two planes written as

$$d = f_1 + f_2 + \Delta \quad (8)$$

where Δ is the adjustable distance between the focus points of two lenses, and f_1 and f_2 are the focuses of *Lens1* and *Lens2* respectively. Besides, A_1, B_1, C_1, and D_1 are given by [16]

$$\begin{bmatrix} A_1 & B_1 \\ C_1 & D_1 \end{bmatrix} = \begin{bmatrix} 1 - \frac{d}{f_1} & d \\ -\frac{1}{f_1} & 1 \end{bmatrix} \quad (9)$$

These are recognized as the transfer matrix elements between the input plane and the front plane of *Lens2*.

Likewise, the integral expression relating the front plane of *Lens2* and the target plane is written as

$$E_2(r_2, L + d) = \frac{i}{\lambda B_2} e^{-ikL} \int_0^{2\pi} \int_0^{a_2} E_1(r_1, d) \cdot e^{-\frac{ik}{2B}\left(A_2 r_1^2 - 2r_2 r_1 \cos(\theta_2 - \theta_1) + D_2 r_2^2\right)} r_1 dr_1 d\theta_1 \quad (10)$$

where E_1 and E_2 are the field distribution at the two planes mentioned above respectively, L stands for the axial working distance of single-beam LDVs, the corresponding transfer matrix is given by

$$\begin{bmatrix} A_2 & B_2 \\ C_2 & D_2 \end{bmatrix} = \begin{bmatrix} 1 - \frac{L}{f_2} & L \\ -\frac{1}{f_2} & 1 \end{bmatrix} \quad (11)$$

The a_2 represents the radius of the transmitted beam on the front plane of the *Lens2*. Here, a lens's effect on a Gaussian beam is relevant. a_2 is provided by [17].

$$a_1 = \sqrt{\frac{(f_1 \cdot a_0)^2}{f_1^2 + Z_0^2}} \quad (12)$$

$$Z_0 = \frac{\pi \cdot a_0^2}{\lambda} \quad (13)$$

$$a_2 = a_1 \cdot \sqrt{1 + \left(\frac{\lambda (d - f_1)}{\pi \cdot a_1^2}\right)^2} \quad (14)$$

The a_1' is the waist radius of Gaussian beam after transformed by the *Lens1*. Z_0 is a parameter corresponding to the waist of input beam.

Further deductions are conducted by taking the spherical aberration into account. This influence is quantified to be a phase factor φ given by

$$\varphi = -ik \cdot SA \cdot r^4 \quad (15)$$

Wherein SA is the spherical aberration coefficient of a lens written as [13]

$$SA = -\frac{1}{32 n_0 (n_0 - 1) f^3} \left[\frac{n_0^3}{n_0 - 1} + (3n_0 + 2)(n_0 - 1) p^2 + \frac{n_0 + 2}{n_0 - 1} q^2 + 4(n_0 + 1) pq \right] \quad (16)$$

where f is the focus of a lens, n_0 is the refractive index of a lens, and p and q are the position and shape factors of a lens respectively. The two quantities are given by

$$p = 1 - \frac{2f}{s'} \quad (17)$$

$$q = \frac{R_2 + R_1}{R_2 - R_1} \quad (18)$$

where s' stands for the image distance from the center of a lens, R_1 and R_2 are the curvatures of the first and second surfaces of a lens respectively.

The spherical aberration is regarded as a new phase term of Eq. (7) and Eq. (10). Hence, the substitution of the phase factor φ into Eq. (7) and Eq. (10) produces

$$E_1(r_1, d) = \frac{i}{\lambda B_1} e^{-ikd} \int_0^{a_1} E_0(r_0, 0) \cdot e^{-ik \cdot SA_{Len1} \cdot r_0^4} \cdot e^{-\frac{ik}{2B}\left(A_1 r_0^2 + D_1 r_1^2\right)} \cdot 2\pi J_0\left(\frac{k}{B_1} r_1 r_0\right) r_0 dr_0 \quad (19)$$

$$E_2(r_2, L + d) = \frac{i}{\lambda B_2} e^{-ikL} \int_0^{a_2} E_1(r_1, d) \cdot e^{-ik \cdot SA_{Len2} \cdot r_1^4} \cdot e^{-\frac{ik}{2B_2}\left(A_2 r_1^2 + D_2 r_2^2\right)} \cdot 2\pi J_0\left(\frac{k}{B_2} r_2 r_1\right) r_1 dr_1 \quad (20)$$

where SA_{Lens1} and SA_{Lens2} stand for the spherical aberration coefficients of *Lens1* and *Lens2*, respectively. J_0 is the zero-order Bessel function. It is possible to look at how a focusing optics module's spherical aberration affects the field distribution of the probe beam using Eqs. (13) and (14).

Since the radius of the probe beam is the distance between the maximum light intensity position and the e^{-2} light intensity position [16], the radius r of the probe beam on the target plane is given by

$$I(r, L + d) = e^{-2} \cdot E_2(0, L + d) \cdot E_2^*(0, L + d) \quad (21)$$

Eq. (21) will be used to determine how the radius of the probe beam varies on the target plane. As a result, based on

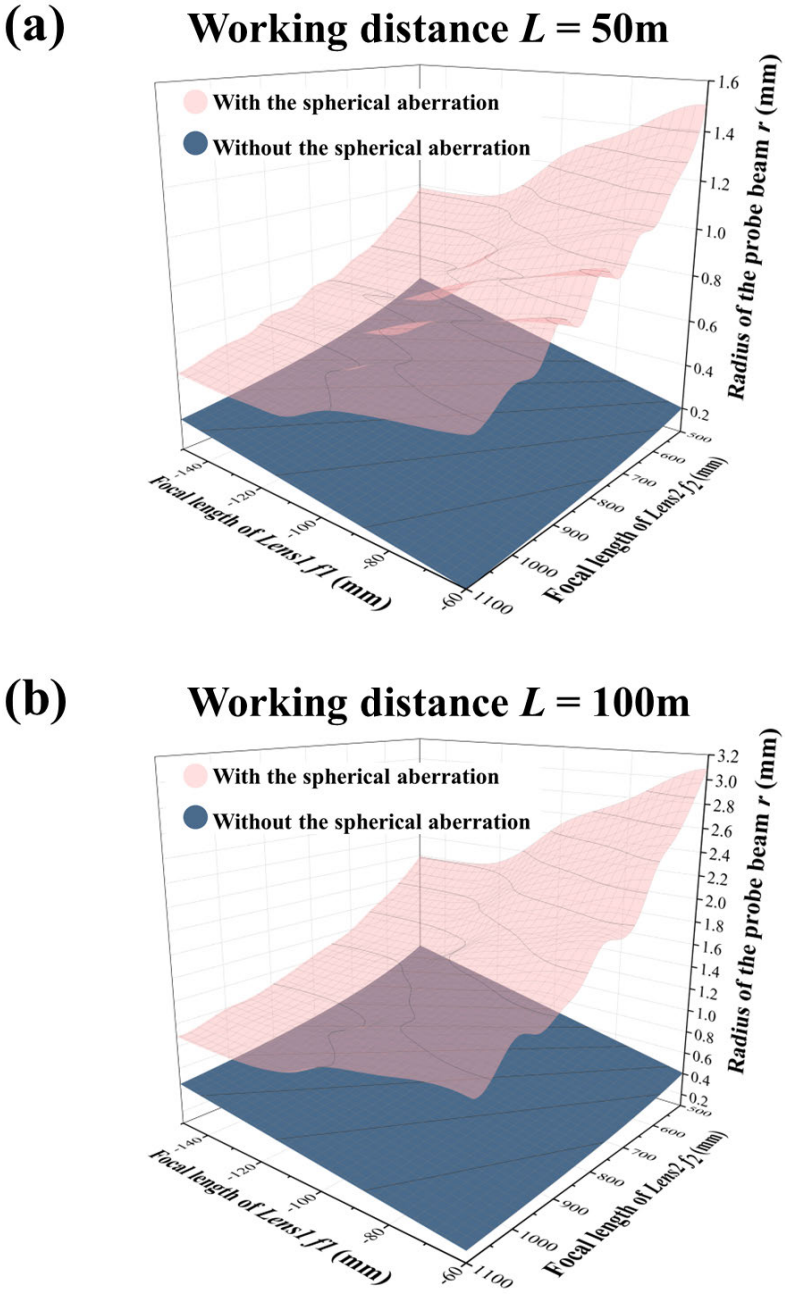

FIGURE 3. The simulation on the variation of the radius of the probe beam after passing through focusing transmitters composed of different Lens1 and Lens2 under two working distances. working distance L = (a)50m and (b)100m.

Eq. (6), more measurable analyses of the effect of spherical aberration on the detection of LDVs are possible.

III. SIMULATION

In this section, simulations are used to examine how spherical aberration affects the measurement of single-beam LDVs. Parameters used in the simulations are listed in the Table 1.

It is assumed that a beam expander collimated and enlarged the probe beam before it entered the optics module. Numerical calculations are used since solving the integral expression of the laser intensity on the target plane analytically is difficult. The field across the input plane is assumed to be

$$E_0(r_0, 0) = \exp\left(-\frac{r_0^2}{w_0^2}\right) \tag{22}$$

TABLE 1. Parameters used in simulations.

Parameters	Quantity
f1	[-150,-60]mm
p1	-1
q1	-1
f2	[500,1100]mm
p2	1
q2	-1
n0	1.51
w0	5mm
λ	532nm

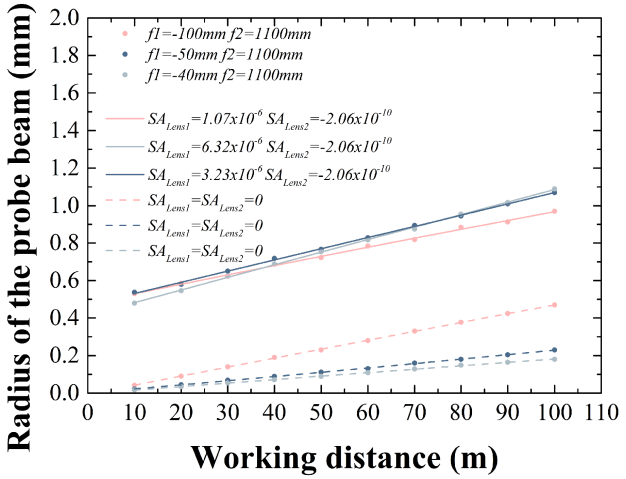

FIGURE 4. The simulation on three different focusing transmitters with or without the influence of spherical aberration.

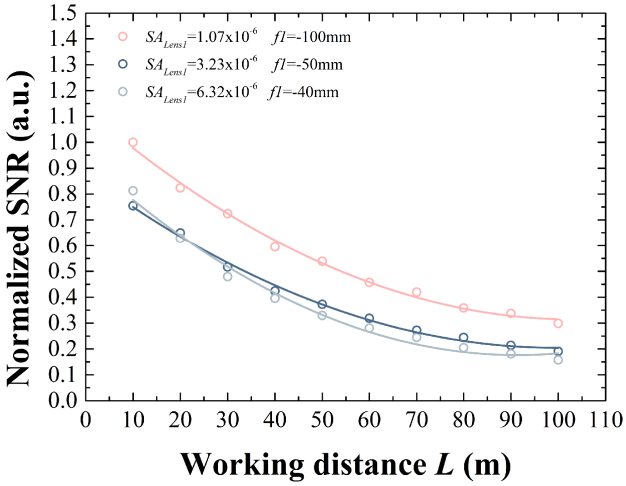

FIGURE 5. Normalized SNR of cases with the spherical aberration.

A. THE VARIATION OF THE RADIUS OF THE PROBE BEAM AFTER PASSING THROUGH DIFFERENT FOCUSING TRANSMITTERS

Fig. 3 shows the variation in the radius of the probe beam at two different working distances. The curve below represents the ideal state without the influence of the spherical aberration, whereas the curve above represents the situation where the spherical aberration is taken into account. It is observed that there is a striking difference between the radius of the probe beam affected by spherical aberration on various target planes and the case without the influence. The spherical aberration effect causes the probe beam's radius to rise, and this variation gets more pronounced as the axial working distance increases.

B. SIMULATION ON LDVS MOUNT WITH SPECIFIC FOCUSING TRANSMITTERS

Three exemplary focused transmitters are used as an example for a clearer explanation. The information about lenses comes from actual specimens in our lab. Simulation results of Fig.4 is based on the parameters listed in Table 2. The three lines in Fig. 4 show that, while *Lens2*'s focal length is fixed, the shorter focus of *Lens1* causes the probe beam's radius to be narrower at the same working distance. This happens when the neglect of spherical aberrations is assumed. However, results that take into account the spherical aberration are radically opposite. As discussed above, it is demonstrated that at greater working distances, the optics module with *Lens1* that has the greatest focus length tends to generate the lowest spot size. This trend can be seen in Fig. 3 as well. Three exemplary focused transmitters are used as an example for a clearer explanation. The information about lenses comes from actual specimens in our lab. The three lines in Fig. 4 show that, while *Lens2*'s focal length is fixed, the shorter focus of *Lens1* causes the probe beam's radius to be narrower at the same working distance. This happens when the neglect of spherical aberrations is assumed. However, results that take into account the spherical aberration are radically opposite. As discussed above, it is demonstrated that at greater working distances, the optics module with *Lens1* that has the greatest focus length tends to generate the lowest spot size. This trend can be seen in Fig. 3 as well.

If other parameters remain constant, Eq. (6) states that the SNR falls as the probe beam's radius increases. This demonstrates the effects of spherical aberration on LDVs. Then, for comparison clarity, the corresponding SNR of cases with spherical aberration is determined. Fig. 5 implies that the SNR of the optics module containing the *Lens1* of the longest focus length outperforms others. Additionally, it demonstrates that when spherical aberration is taken into account, the SNR of the measurement of LDVs suffers significantly and rapidly with an increase in working distance.

The findings highlight the importance of carefully considering the impact of spherical aberration while designing the optics for LDVs, particularly the one for remote velocity measurement.

IV. EXPERIMENTS

The experimental test of the simulation is demonstrated in this section. The integrated single-beam LDV structure, which includes a velocity measurement module and a focusing

TABLE 2. Parameters used in simulations.

	Transmitter 1	Transmitter 2	Transmitter 3
f1	-100	-50	-40
p1	-1	-1	-1
q1	-1	0	0
f2	1100	1100	1100
p2	1	1	1
q2	-1	-1	-1
n0	1.5	1.5	1.5
w0	5	5	5
λ	532	532	532
SA_{LENS1}	$1.07\text{x}10^{-6}$	$3.23\text{x}10^{-6}$	$6.32\text{x}10^{-6}$
SA_{LENS2}	$-2.06\text{x}10^{-10}$	$-2.06\text{x}10^{-10}$	$-2.06\text{x}10^{-10}$

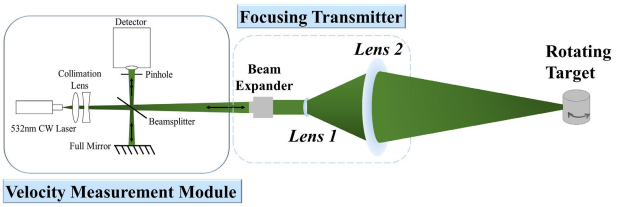

FIGURE 6. Experimental setup.

TABLE 3. Main characteristics of experiments.

Power of the probe beam	The wavelength of the probe beam	The ratio of the beam expander	*Lens* 2	*Lens* 1	Utilized in
100mW	532nm	5x	1100mm	-100mm -50mm -40mm	Section 4.3
			500mm	-150mm	Section 4.2

transmitter, is shown in Fig. 6. The beam from CW laser is divided into the probe beam and the reference beam by the beam splitter. The probe beam is expanded by a beam expander before focused to a concrete cylinder by the focusing transmitter. The cylinder in motion is the intended target. The scattered light from rotating cylinder surface mixing with the reference beam on the detector produces beat signal containing Doppler information. Table 3 shows the list of the key traits.

A. PRACTICAL STANDARD FOR THE EVALUATION OF THE PERFORMANCE OF SINGLE-BEAM LDVS

For convenience, the signal quality factor is used in this article in place of SNR to quantify the performance of the measurement of single-beam LDVs. After the target's scattering light is identified and transformed into an electrical signal, FFT is applied to the signal to get the signal's spectrum. When the target plane is stationary, the spectrum in this instance is recorded as the single-beam LDV's noisy background spectrum and normalized across the whole range. Given that the target plane is moving, it is easy to see a peak in the signal's spectrum at the Doppler frequency associated with the target plane's velocity. The intensity of the Doppler frequency divided by the intensity of the corresponding frequency point in the normalized noise background spectrum is therefore used to determine the signal quality factor. This factor is theoretically equivalent to the SNR and has good simplicity and technical applicability for assessing the measurement of single-beam LDVs.

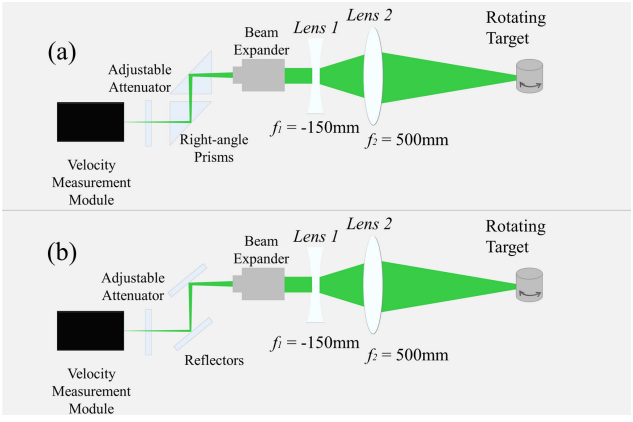

FIGURE 7. Setups for the comparison experiment(a)with and (b) without right-angle prisms.

B. EXPERIMENTAL DEMONSTRATION OF THE INFLUENCE OF SPHERICAL ABERRATION

If the incident beam is not collimated, a plane-parallel plate in the optical path also introduces spherical aberration [13].

Note that the aberration increases linearly with the thickness of the plate. To demonstrate how spherical aberration affects the measurement of single-beam LDVs, a comparison experiment is created. A right-angle prism is equivalent to a plane-parallel plate with a thickness equal to the length of the optical path in which the incident beam travels in the prism. As seen in Fig. 7, in comparison to the control group, a few right-angle prisms are added between the measuring and optics modules. Prisms reflect the probe beam before it is collimated and introduce extra spherical aberration. An adjustable attenuator adjusts the power of the probe beam in two groups to be equal. Working distance is kept fixed.

The comparison of signal quality factors measured in two groups is presented in Fig. 8. Additionally, a beam spot analyzer takes two images of the cross-section of the probe beam on the target plane in Fig. 9. Due to additional spherical aberration, the group using right-angle prisms estimates the target's velocity with an extended probe beam. When the other parameters remain fixed, the SNR of LDV rapidly decreases as the radius of the probe beam increases. It is the process by which spherical aberration affects how LDVs are measured.

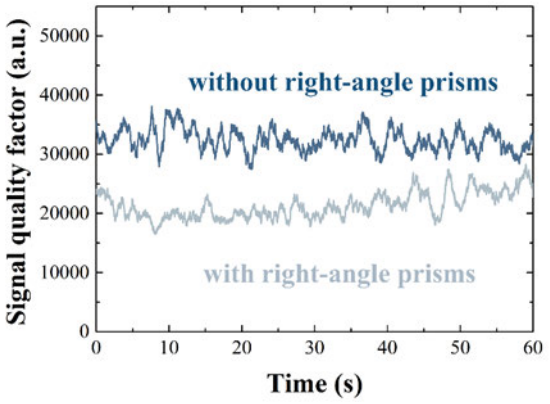

FIGURE 8. Signal quality factors measured in the comparison experiment.

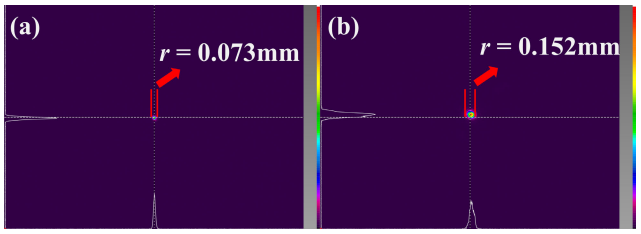

FIGURE 9. Two pictures of the cross-section of the probe beam on the target plane (a)without right-angle prisms, and (b) with right-angle prisms in the optical path.

C. EXPERIMENTS ON LDVS MOUNTED WITH DIFFERENT OPTICAL MODULES

Fig. 10 is one picture of the experimental site. The axial working distance between the rotating target and the LDV is fixed at 100m. Figure 11 shows the signal quality metrics obtained from the LDV equipped with various optics modules. The parameters of these modules match simulations.

The greater signal quality is achieved when the focal length of Len1 is longer when the focal length of Lens2 is kept unchanged. In other words, it causes the measurement of the LDV to have a higher SNR.

Considering the signal quality factor varying with the working distance, a group of signal quality factor data is measured by the LDV mounted with an optical module composed of Lens1 -100mm and Lens2 1100mm. Data are measured every ten meters. The results are shown in Fig. 12, and the falling trend corresponds to what Eq. (20) predicted. It is also confirmed that the expression of SNR for LDVs is correct.

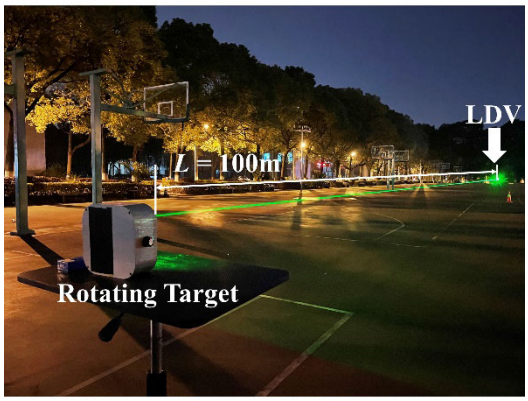

FIGURE 10. The picture of the field campaign.

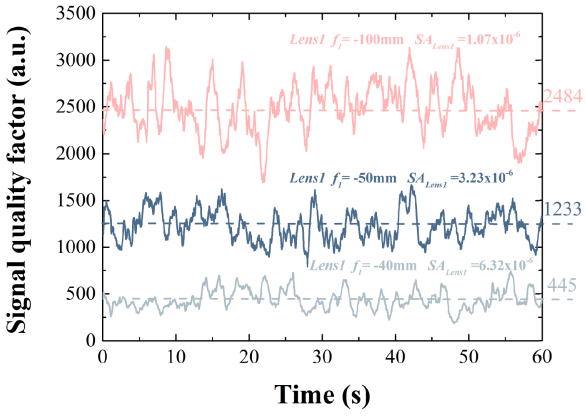

FIGURE 11. Signal quality factors measured by the LDV exploiting different optics modules; The average for every group is listed next to the figure.

All these experimental results are virtually in agreement with the simulations in section III and verify the validity of the theory developed in this paper. All of these experimental findings essentially concur with the simulations in section III and support the hypothesis put out in this work.

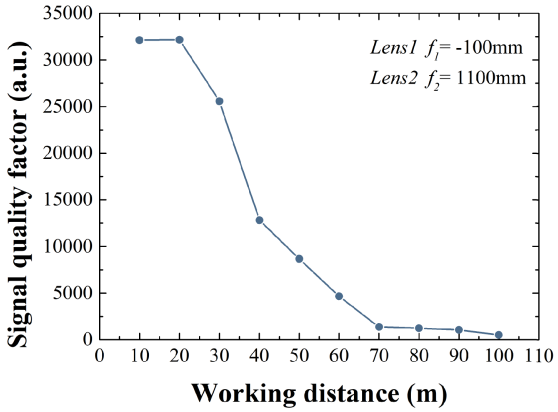

FIGURE 12. Signal quality factors measured by the LDV vary with the working distance.

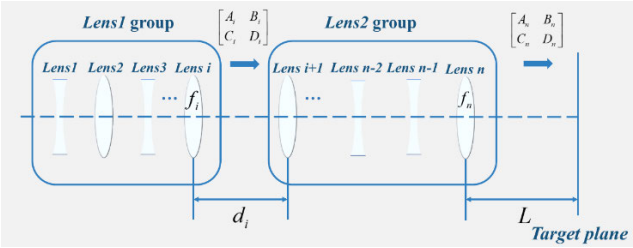

FIGURE 13. The case that the focusing optics are composed of more than two lenses.

V. GENERALIZATION ANALYSIS

In general, it is noted that either *Lens1* or *Lens2* in the focusing optics can be replaced in function by a set of lenses if the equivalent focal length is the same as *Lens1* or *Lens2*. Fig. 13 depicts the case that the focusing optics are composed of more than two lenses. It is suggested to adapt the analysis technique presented in section II to complex optics. Given below is a generalization of the field distribution on *Lens i*'s front plane.

$$\begin{aligned} &E_i\left(r_i, d_1+\cdots+d_i\right) \\ &\quad=\frac{i}{\lambda B_i}\exp(-ikd_i)\int_0^{a_i} E_{i-1}(r_{i-1}, d_1+\cdots+d_i) \\ &\qquad\times\exp(-ik\cdot SA_{Lens\,i}\cdot r_{i-1}^4)\exp[\frac{-ik}{2B_i}(A_i r_{i-1}^2+D_i r_i^2)] \\ &\qquad\cdot 2\pi J_0\left(\frac{k}{B_i}r_i r_{i-1}\right) r_{i-1}dr_{i-1}\ (i\le n-1) \end{aligned} \tag{23}$$

where n is the total amount of lenses in the focusing optics, a_i represents the radius of the transmitted beam on the front plane of *Lens i*, d_i stands for the distance between *Lens i+1* and *Lens i*, SA_{Lensi} represents the spherical aberration coefficient of *Lens i*, the corresponding transfer matrix is given by

$$\begin{bmatrix} A_i & B_i \\ C_i & D_i \end{bmatrix} = \begin{bmatrix} 1-\frac{d_i}{f_i} & d_i \\ -\frac{1}{f_i} & 1 \end{bmatrix} \tag{24}$$

where f_i is the focal length of *Lens i*. the field distribution and light intensity distribution on the target plane are given by

$$\begin{aligned} &E_n\left(r_n, d_1+\cdots+d_{n-1}\right) \\ &\quad=\frac{i}{\lambda B_n}\exp(-ikL)\int_0^{a_n} E_{n-1}(r_{n-1}, d_1+\cdots+d_n) \\ &\qquad\times\exp(-ik\cdot SA_{Lens\,n}\cdot r_{n-1}^4)\exp[\frac{-ik}{2B_n}(A_n r_{n-1}^2+D_n r_n^2)] \\ &\qquad\cdot 2\pi J_0\left(\frac{k}{B_n}r_n r_{n-1}\right) r_{n-1}dr_{n-1} \end{aligned} \tag{25}$$

$$\begin{aligned} &I\left(r_n, L+d_1+\cdots+d_{n-1}\right) \\ &\quad=E_n\left(r_n, L+d_1+\cdots+d_{n-1}\right)\cdot E_n^*\left(r_n, L+d_1+\cdots+d_{n-1}\right) \end{aligned} \tag{26}$$

where L is the working distance of single-beam LDVs, SA_{Lensn} represents the spherical aberration coefficient of *Lens n*, a_n represents the radius of the transmitted beam on the front plane of the *Lens n* which is calculated like a_2 in section II,the corresponding transfer matrix is written as

$$\begin{bmatrix} A_n & B_n \\ C_n & D_n \end{bmatrix} = \begin{bmatrix} 1-\frac{L}{f_n} & L \\ -\frac{1}{f_n} & 1 \end{bmatrix} \tag{27}$$

Fig. 14 demonstraes the summary of the approach provided in this paper for evaluating and optimizing the performance of single-beam LDV used for distant velocity measurement. Consequently, regardless of how complex the optics in single-beam LDVs are, the radius of the probe beam on the target plane is easily studied while the performance of LDVs is also assessed.

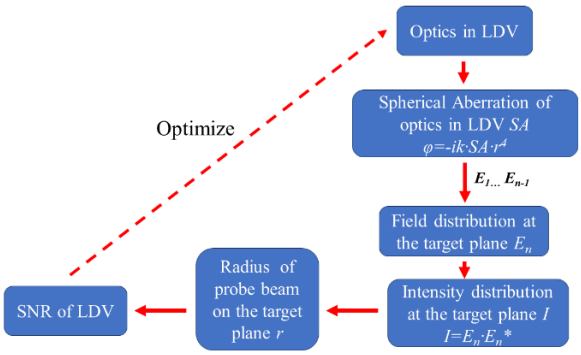

FIGURE 14. Diagram of the approach provided in this manuscript for evaluating and enhancing the SNR performance of single-beam LDV utilized for long-range velocity measurements.

VI. DISCUSSION

As was previously stated, whether in theoretical analysis or actual test, the spherical aberration of optics has a substantial impact on the measurement of single-beam LDVs. These findings are explained by the fact that light rays that illuminate the lens surface off-center are refracted more or less than those that do so near the center. This distortion prevents the LDV probe beam from being sufficiently focused on the target plane. Consequently, the SNR of single-beam

LDVs is reduced. The SNR in this instance for the remote velocity measurement is significantly lower than that for the measurement for near working distances. The spherical aberration of optics will deteriorate measurement results further. So it is crucial to take spherical aberration into account while building the LDVs' focusing transmitter for remote velocity measurement.

ACKNOWLEDGMENT

The authors would like to express their gratitude to EditSprings (https://www.editsprings.cn) for the expert linguistic services provided.

REFERENCES

[1] J. Zhou, X. Nie, and J. Lin, "A novel laser Doppler velocimeter and its integrated navigation system with strapdown inertial navigation," *Opt. Laser Technol.*, vol. 64, pp. 319–323, Dec. 2014, doi: 10.1016/j.optlastec.2014.06.001.

[2] X. Zhang, J. Yin, Z. Lin, and C. Zhang, "A positioning and orientation method based on the usage of INS and single-beam LiDAR," *Optik*, vol. 126, no. 22, pp. 3376–3381, Nov. 2015, doi: 10.1016/j.ijleo.2015.06.066.

[3] Q. Wang, X. Nie, C. Gao, J. Zhou, G. Wei, and X. Long, "Calibration of a three-dimensional laser Doppler velocimeter in a land integrated navigation system," *Appl. Opt.*, vol. 57, no. 29, p. 8566, 2018, doi: 10.1364/ao.57.008566.

[4] R. Huang, X. Nie, and J. Zhou, "Laser Doppler velocimeter and its calibration system," *Measurement*, vol. 134, pp. 286–292, Feb. 2019, doi: 10.1016/j.measurement.2018.10.084.

[5] Z. Xiang, Q. Wang, R. Huang, C. Xi, X. Nie, and J. Zhou, "In-motion initial alignment method for a laser Doppler velocimeter-aided strapdown inertial navigation system based on an adaptive unscented quaternion H-infinite filter," *Meas. Sci. Technol.*, vol. 33, no. 3, Mar. 2022, Art. no. 035001, doi: 10.1088/1361-6501/ac37e9.

[6] Q. Pentek, P. Kennel, T. Allouis, C. Fiorio, and O. Strauss, "A flexible targetless LiDAR–GNSS/INS–camera calibration method for UAV platforms," *ISPRS J. Photogramm. Remote Sens.*, vol. 166, pp. 294–307, Aug. 2020, doi: 10.1016/j.isprsjprs.2020.05.014.

[7] E. Petritoli and F. Leccese, "Improvement of altitude precision in indoor and urban canyon navigation for small flying vehicles," in *Proc. IEEE Metrol. Aerosp. (MetroAeroSpace)*, Jun. 2015, pp. 56–60.

[8] K.-W. Chiang, G.-J. Tsai, Y.-H. Li, and N. El-Sheimy, "Development of LiDAR-based UAV system for environment reconstruction," *IEEE Geosci. Remote Sens. Lett.*, vol. 14, no. 10, pp. 1790–1794, Oct. 2017, doi: 10.1109/LGRS.2017.2736013.

[9] L. Chen, J. Zhou, X. Nie, and S. Jin, "Measurement range expansion of single-beam laser Doppler velocimeter based on a focusing transmitter," *Optik*, vol. 272, Feb. 2023, Art. no. 170383.

[10] A. E. Siegman, "Analysis of laser beam quality degradation caused by quartic phase aberrations," *Appl. Opt.*, vol. 32, no. 30, p. 5893, 1993.

[11] J. Pu and H. Zhang, "Intensity distribution of Gaussian beams focused by a lens with spherical aberration," *Opt. Commun.*, vol. 151, nos. 4–6, pp. 331–338, 1998, doi: 10.1016/s0030-4018(98)00097-2.

[12] A. A. Alkelly, H. Al-Nadary, and I. A. Alhijry, "The intensity distribution of hollow Gaussian beams focused by a lens with spherical aberration," *Opt. Commun.*, vol. 284, no. 1, pp. 322–329, Jan. 2011, doi: 10.1016/j.optcom.2010.08.040.

[13] V. N. Mahajan, *Aberration Theory Made Simple*, 2nd ed. USA: SPIE, 2011.

[14] T. Fujii, *Laser Remote Sensing*. Boca Raton, FL, USA: CRC Press, 2005.

[15] S. A. Collins, "Lens-system diffraction integral written in terms of matrix optics," *J. Opt. Soc. Amer.*, vol. 60, no. 9, p. 1168, 1970, doi: 10.1364/josa.60.001168.

[16] J. Alda, *Encyclopedia of Optical Engineering: Laser and Gaussian Beam Propagation and Transformation*, R. G. Driggers, Ed. New York, NY, USA: Marcel Dekker, 2003, pp. 999–1013.

[17] S. Nemoto, "Transformation of Waist parameters of a Gaussian beam by a thick lens," *Appl. Opt.*, vol. 29, no. 6, p. 809, 1990.

LANJIAN CHEN received the B.E. and M.S. degrees from the National University of Defense Technology (NUDT), Changsha, China, in 2017 and 2019, respectively, where he is currently pursuing the Ph.D. degree with the College of Advanced Interdisciplinary Studies.

His current research interest includes airborne laser Doppler velocimeter.

JIAN ZHOU received the Ph.D. degree in optical engineering from the National University of Defense Technology (NUDT), Changsha, China, in 2011.

He is currently an Associate Professor with the College of Advanced Interdisciplinary Studies, NUDT. His current research interests include laser Doppler velocimeter technology and applications of LDV in navigation and localization.

CHONGBIN XI received the B.E. degree from Chongqing University (CQU), Chongqing, China, in 2018, and the M.S. degree from the National University of Defense Technology (NUDT), Changsha, China, in 2020, where he is currently pursuing the Ph.D. degree with the College of Advanced Interdisciplinary Studies.

His current research interest includes laser Doppler velocimeter technology.

XIAOMING NIE received the Ph.D. degree in optical engineering from the National University of Defense Technology (NUDT), Changsha, China, in 2014.

He is currently an Associate Professor with the College of Advanced Interdisciplinary Studies, NUDT. His current research interests include laser Doppler velocimeter technology and applications of LDV in navigation and localization.

SHILONG JIN received the Ph.D. degree from the National University of Defense Technology (NUDT), Changsha, China.

He is currently a Professor with the College of Advanced Interdisciplinary Studies, NUDT. His current research interest includes laser gyroscope.